

The demographic history of populations experiencing asymmetric gene flow: combining simulated and empirical data

I. PAZ-VINAS,*†‡ E. QUÉMÉRÉ,§ L. CHIKHI,†‡¶ G. LOOT*‡ and S. BLANCHET*†

*Centre National de la Recherche Scientifique (CNRS), Station d'Écologie Expérimentale du CNRS à Moulis, USR 2936, Moulis F-09200, France, †Centre National de la Recherche Scientifique (CNRS), Université Paul Sabatier, École Nationale de Formation Agronomique (ENFA), UMR 5174 EDB (Laboratoire Évolution & Diversité Biologique), 118 route de Narbonne, Toulouse cedex 4, F-31062, France, ‡Université de Toulouse, UPS, UMR 5174 (EDB), 118 route de Narbonne, Toulouse cedex 4, F-31062, France, §Institut National de la Recherche Agronomique (INRA), UMR Comportement et Écologie de la Faune Sauvage, INRA, BP 52627, Castanet-Tolosan cedex, F-31326, France, ¶Instituto Gulbenkian de Ciência, Rua da Quinta Grande 6, Oeiras P-2780-156, Portugal

Abstract

Population structure can significantly affect genetic-based demographic inferences, generating spurious bottleneck-like signals. Previous studies have typically assumed island or stepping-stone models, which are characterized by symmetric gene flow. However, many organisms are characterized by asymmetric gene flow. Here, we combined simulated and empirical data to test whether asymmetric gene flow affects the inference of past demographic changes. Through the analysis of simulated genetic data with three methods (i.e. BOTTLENECK, M-ratio and MSVAR), we demonstrated that asymmetric gene flow biases past demographic changes. Most biases were towards spurious signals of expansion, albeit their strength depended on values of effective population size and migration rate. It is noteworthy that the spurious signals of demographic changes also depended on the statistical approach underlying each of the three methods. For one of the three methods, biases induced by asymmetric gene flow were confirmed in an empirical multispecific data set involving four freshwater fish species (*Squalius cephalus*, *Leuciscus burdigalensis*, *Gobio gobio* and *Phoxinus phoxinus*). However, for the two other methods, strong signals of bottlenecks were detected for all species and across two rivers. This suggests that, although potentially biased by asymmetric gene flow, some of these methods were able to bypass this bias when a bottleneck actually occurred. Our results show that population structure and dispersal patterns have to be considered for proper inference of demographic changes from genetic data.

Keywords: ABC, demographic change, fish, rivers, source–sink dynamics

Received 4 April 2012; revision received 5 March 2013; accepted 11 March 2013

Introduction

Inferring the demographic history of populations such as changes in effective population size (contractions, expansions) is of prime importance for basic research and conservation issues (Chikhi & Bruford 2005; Leblois *et al.* 2006). Several indirect methods based on the anal-

ysis of neutral genetic variation have been developed to that aim (Cornuet & Luikart 1996; Beaumont 1999; Garza & Williamson 2001; Storz & Beaumont 2002). These methods have been largely used to assess the impact of environmental or anthropogenic changes on the demographic history of endangered populations (e.g. Goossens *et al.* 2006; Sousa *et al.* 2008).

However, inferring the demographic history of wild populations remains challenging. Indeed, most methods assume that populations can be approximated

Correspondence: Ivan Paz-Vinas, Fax: (0033)561557327; E-mail: ivanpaz23@gmail.com

by simple models such as the Wright–Fisher model (Cornuet & Luikart 1996; Leblois *et al.* 2006). However, wild populations rarely match these assumptions, because most of them are either spatially structured, affected by external gene flow and/or at a nonequilibrium state (Hanski 1998; Broquet *et al.* 2010; Chikhi *et al.* 2010). Consequently, any deviations from these simple models may lead to misinterpretations or incorrect inferences (Nielsen & Beaumont 2009; Städler *et al.* 2009; Chikhi *et al.* 2010). Given that the development of inference methods based on complex demographic models poses problems of its own, it is crucial to explore how existing inference methods are robust to deviations from simple models assumptions (Leblois *et al.* 2006; Städler *et al.* 2009; Chikhi *et al.* 2010). Recent programs based on the coalescent framework (Kingman 1982) allow the simulation of genetic data under a wide variety of population models (Hoban *et al.* 2012). Thus, specific simulated genetic data sets can be analysed to test the potential effects of particular population characteristics on the genetic inference of populations' demographic history. Accordingly, population structure (Nielsen & Beaumont 2009; Städler *et al.* 2009; Chikhi *et al.* 2010; Peter *et al.* 2010), sampling scheme (Städler *et al.* 2009; Chikhi *et al.* 2010), gene flow reductions (Broquet *et al.* 2010) and isolation by distance (Leblois *et al.* 2006) have been identified as generators of false signals of demographic change, with biases towards bottlenecks (e.g. Broquet *et al.* 2010; Chikhi *et al.* 2010) and, more rarely, towards expansions (e.g. Leblois *et al.* 2006).

A population characteristic that has rarely been considered to date in the context of demographic history inferences is asymmetric gene flow. Differences in habitat quality, social interactions or abiotic constraints (e.g. wind, oceanic currents, river flow or gravity) frequently generate source–sink dynamics and impose asymmetric gene flow on natural populations (Kawecki & Holt 2002). For instance, in riverine freshwater ecosystems, organisms generally experience an inherent downstream-biased gene flow due to the unidirectional water flow of rivers (Hänfling & Weetman 2006; Pollux *et al.* 2009). Such asymmetry in gene flow drastically affects the genetic structure of wild riverine populations, with, for instance, an accumulation of genetic diversity (e.g. number of alleles per locus) downstream (i.e. sink populations, Kawecki & Holt 2002; Hänfling & Weetman 2006).

The demography of wild populations is dramatically affected by human pressures and notably by human-induced habitat fragmentation (Fahrig 2003; Henle *et al.* 2004). Freshwater ecosystems are particularly affected by habitat fragmentation, either through the building of hydroelectric dams or the presence of smaller obstacles

like weirs (2–3 m high, Raeymaekers *et al.* 2008; Blanchet *et al.* 2010). In general, habitat fragmentation induces changes in effective population size (N_e) that are theoretically inferable using the methods described above. However, river fragmentation by dams and weirs may strongly affect the movements of fishes, in both upstream and downstream directions. As a result, river fragmentation can alter natural gene flow, either by exacerbating or, on the contrary, by disrupting the natural asymmetric (i.e. downstream-biased) gene flow expected on such ecosystems (Hänfling & Weetman 2006; Raeymaekers *et al.* 2008; but see Horreo *et al.* 2011). Although several studies have used coalescent- and frequency-based estimators of N_e in fragmented rivers to infer effects of recent fragmentation (Alò & Turner 2005; Sousa *et al.* 2008; Nock *et al.* 2011), none of them have quantified how asymmetric gene flow might affect the inference of past demographic changes that can be drawn from molecular markers in such ecosystems.

In this article, we explored both theoretically and empirically the potential problem posed by asymmetric gene flow to infer temporal changes in N_e . First, we analysed genetic data simulated under a stationary linear stepping-stone model to test whether asymmetric gene flow can generate false signals of demographic changes. This was done using three methods widely used to infer demographic changes: those implemented in the programs BOTTLENECK (Cornuet & Luikart 1996; Piry *et al.* 1999) and MSVAR 1.3 (Beaumont 1999; Storz & Beaumont 2002) and the M-ratio method (Garza & Williamson 2001). Second, we used the same three methods to analyse empirical data involving four freshwater fish species (*Squalius cephalus*, *Leuciscus burdigalensis*, *Gobio gobio* and *Phoxinus phoxinus*) sampled in two rivers, which differ by their level of anthropogenic fragmentation and asymmetric gene flow.

Materials and methods

Simulated data

To explore the consequences of asymmetric gene flow on the inference of changes in N_e , we simulated genetic data under 27 different scenarios representing populations experiencing symmetric or asymmetric gene flow, but no changes in N_e , and then used this data as input for three methods used to infer changes in N_e .

The population genetics model. We used the coalescent-based program ms along with the microsat.exe program (Hudson 2002) to simulate genetic data under a strict stepwise-mutation model (SMM). Specifically, we approximated a river, by considering a linear stepping-

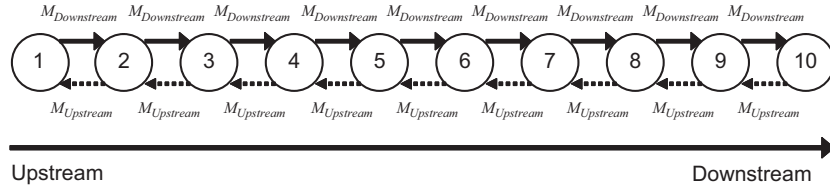


Fig. 1 Diagram representing the linear stepping-stone model with asymmetric gene flow. Black circles are demes. $M_{\text{Downstream}}$ characterizes downstream-directed gene flow, while M_{Upstream} indicates upstream-directed gene flow. Here, deme one is considered as the most upstream deme of a hypothetical river.

stone population model composed of 10 demes (see Fig. 1). All demes had the same effective number of diploid individuals N , which remained constant across generations. Each deme was characterized by three parameters: the scaled mutation rate $\theta = 4N\mu$, where μ represents the neutral mutation rate *per locus*, and two scaled migration rates (M) corresponding to the downstream- and upstream-directed gene flow: $M_{\text{Downstream}} = 4Nm$ and $M_{\text{Upstream}} = \frac{M_{\text{Downstream}}}{a}$, where m is the migration rate and a is a parameter representing the gene flow asymmetry (Fig. 1). We used values of $a > 1$ to generate downstream-biased gene flow. Deme 1 and deme 10 in Fig. 1 can be considered as the most upstream and downstream demes of the hypothetical river, respectively.

Parameter estimation and exploration. For all simulations, we assumed a unique neutral mutation rate of $\mu = 5.56 \times 10^{-4}$. This value corresponds to the average mutation rate calculated for 49 microsatellite loci in the cyprinid fish *Cyprinus carpio L.* (Yue *et al.* 2007). For selecting values for all other model parameters (i.e. N , m and a , this combination of parameters will hereafter be referred to ϕ), we first estimated values that best characterize riverine fish populations by performing ABC-regression analyses (i.e. approximate Bayesian computation, Beaumont *et al.* 2002) based on observed summary statistics compiled for several populations through a literature survey (Table S1, Supporting information). Specifically, we first obtained or computed for sixteen riverine fish populations from fourteen rivers (i) the mean allelic richness *per population* (AR) and (ii) the Pearson's correlation coefficient (r) between the mean AR *per sampling location* and the distance of each sampling location from the river source. Significant positive correlations between AR and distance from the river source are characteristic of river organisms that experience downstream-biased gene flow asymmetry (Hänfling & Weetman 2006; Blanchet *et al.* 2010). In a second step, we generated a total of 1 328 784 different genetic data sets under the population genetics model described above, by drawing values for ϕ from grids, as in Weiss & von Haeseler (1998; see Fig. S1, Support-

ing information). As noted by Beaumont *et al.* (2002), grids of parameters can be seen as uniform priors. For each genetic data set, fifteen independent microsatellite loci were simulated, and a total of 22 diploid individuals were sampled for each deme. As for the literature survey populations, two summary statistics (AR and r) were computed for each simulated data set.

Next, we applied an ABC-regression algorithm (Beaumont *et al.* 2002) to each surveyed population independently, by using the R package 'ABC' (Csillery *et al.* 2012). For each ABC analysis, we retained 1% of the simulations whose summary statistics were the closest from those calculated for the surveyed population. Imperfect matching between observed and simulated data was corrected by using a local linear regression method (Beaumont *et al.* 2002; Csillery *et al.* 2012). We estimated the median values of ϕ from the corrected posterior distributions of ϕ for each population (see Table S1, Supporting information) and, finally, we averaged these median values over all surveyed populations to obtain a first set of ϕ values: $N = 3147$, $m = 0.053$ and $a = 7.5$ (Table S1, Supporting information). We assumed that this set of ϕ values approximately characterizes riverine fish populations. Then, to explore and generalize the effects of varying N , m and a on the inference of changes in N_e , we explored two additional values *per parameter* [leading to exploring $N = (50, 500, 3147)$, $m = (0.01, 0.053, 0.1)$ and $a = (1, 7.5, 50)$] and crossed all parameter values in a full-factorial design so as to generate genetic data under 27 different scenarios. An asymmetry of $a = 50$ is probably unrealistic, but the goal here was to explore the effect of asymmetry in extreme conditions so as to explore how it differs from a more realistic scenario (i.e. $a = 7.5$). These scenarios were used to generate input genetic data for further demographic history analyses (see section Demographic history inference).

Empirical data

Biological models. The four fish species considered here are all of the family Cyprinidae, belong to the same trophic level (i.e. they are essentially insectivorous) and

differ principally in their maximum body length and dispersal abilities (Bolland *et al.* 2008; De Leeuw & Winter 2008). *Squalius cephalus* (the European chub) and *Leuciscus burdigalensis* (the rostrum dace) are two large-bodied fish (a maximum body length of 600 mm and 400 mm, respectively), whereas *Gobio gobio* (the gudgeon) and *Phoxinus phoxinus* (the European minnow) are small-bodied fish (200 mm and 140 mm, respectively).

Study area. Sampling was performed in two rivers that belong to the Adour-Garonne basin drainage (south-western France): the Célé and the Viaur rivers (Fig. S2, Supporting information). These rivers present similar abiotic conditions but display differences concerning their level of fragmentation. The Viaur River is highly fragmented with more than 50 small weirs (2–3 m high, constructed within the last 800 years) and two recent hydroelectric dams (30 m high, dating from 60 years ago, see Fig. S2, Supporting information). We henceforth refer to this river as the ‘highly fragmented river’. In the Célé River, ten-fifteen small weirs are found along the river gradient. These were established over the last century and most of them are equipped with fish ladders. The Célé River will be referred to as the ‘weakly fragmented river’. It is noteworthy that asymmetric gene flow, effective population size and migration rate values have been estimated for all these populations (i.e. a population here refers to a species within a river system) through the ABC-regression algorithms presented above; these eight empirical populations are characterized by a wide range of parameter values (see Table S1, Supporting information).

Sampling design. During summer 2006, a total of 10 and 11 sites were sampled on the Viaur and Célé rivers, respectively (Fig. S2, Supporting information). We covered the entire upstream–downstream gradient for both rivers to account for the entire genetic structure of the fish populations. At each site, about 20 individuals *per* species were sampled by electric fishing. Small fragments of pelvic fins were collected and preserved in 70% ethanol for later genetic analyses. *L. burdigalensis* and *S. cephalus* were not found in all sampling sites, probably because the habitat (notably temperature) is not favourable for these two species.

Genetic data. A salt-extraction protocol (Aljanabi & Martinez 1997) was performed to extract genomic DNA from the pelvic fins of fishes. *Phoxinus phoxinus* and *G. gobio* were genotyped at eight microsatellite loci, *Squalius cephalus* at ten loci and *Leuciscus burdigalensis* at fifteen loci. Loci were amplified using multiplex PCRs and amplified fragments were scored using the software

GENEMAPPER® v.4.0 (Applied Biosystems, Foster City, CA, USA). Neither departure from Hardy–Weinberg equilibrium nor null alleles were detected for any of these loci (see Blanchet *et al.* 2010 for further details).

Demographic history inference

We used three approaches to infer past demographic changes through the analysis of genetic data. Two of them are moment-based methods that rely on summary statistics (i.e. the BOTTLENECK method, Cornuet & Luikart 1996; and the M-ratio method, Garza & Williamson 2001) and the third uses a full-likelihood Bayesian approach (i.e. the MSVAR method, Beaumont 1999; Storz & Beaumont 2002). For simulated data, analyses were performed at two different spatial levels: (i) at the deme level, where each deme was analysed independently (i.e. 10 demes \times 27 scenarios = 270 analyses, 22 individuals per analysis), and (ii) at the population level, where all individuals from a same scenario were pooled together in a single analysis (i.e. one analysis per scenario, 220 individuals per analysis). Pooling individuals from multiple sampling locations counters potential biases induced by population structure when looking for demographic changes and improves the characterization of parameters associated with demographic changes at the population level (Chikhi *et al.* 2010). Due to the computational burden inherent to MSVAR, population-level analyses were not performed using this method. For empirical data, analyses were carried out (i) at the sampling site level (i.e. 74 analyses, ~20–22 individuals *per* analysis) and (ii) at the population level (i.e. eight analyses, between 140 and 220 individuals *per* analysis).

BOTTLENECK method. We applied the moment-based method of Cornuet & Luikart (1996) as implemented in the BOTTLENECK software (Piry *et al.* 1999). This method compares the expected heterozygosity computed from a sample (H_e) through observed allele frequencies with the expected heterozygosity (H_{eq}) based on the allele frequencies expected at the mutation–drift equilibrium (given the observed number of alleles n_A of the sample). The significance of deviations from mutation–drift equilibrium was tested through Wilcoxon’s signed rank tests. For simulated data, we performed analyses assuming the stepwise-mutation model (SMM, Piry *et al.* 1999), as it is the mutation model used by ms to simulate the data (Hudson 2002). Additionally, we calculated from the output of BOTTLENECK departures from mutation–drift equilibrium averaged over loci: $\Delta H = H_e - H_{eq}$ (Broquet *et al.* 2010). For empirical data, we performed analyses assuming a two-phase mutation model (TPM), which is more appropriate for empirical

microsatellite data (Di Rienzo *et al.* 1994; Piry *et al.* 1999). We parameterized the TPM with 90% single-step mutations (Garza & Williamson 2001), assuming a conservative variance among multiple steps of 10.

M-ratio method. To detect significant population declines in our data sets, we applied Garza and Williamson's M-ratio test (Garza & Williamson 2001). It is noteworthy that this method (contrary to the two other methods) does not allow the detection of demographic expansions. In bottlenecked populations, the number of alleles on microsatellite loci (n_A) is expected to be reduced more quickly than the range in allele size (r_A). As a result, the ratio $M = n_A/r_A$ will be smaller in bottlenecked populations than in stable populations (Garza & Williamson 2001). Accordingly, we calculated M for both empirical and simulated data sets. Then, we compared M values obtained from our data with 95% critical M values (M_c), calculated from 10 000 simulations of stable populations with the Critical_M program (Garza & Williamson 2001). An M value that falls below the M_c value indicates that the population has experienced a significant bottleneck. For simulated scenarios, we assessed M_c values assuming the SMM, and using the θ values previously used to simulate the data. For empirical data, θ was calculated assuming $\mu = 5.56 \times 10^{-4}$ and using N_e values reported in Blanchet *et al.* (2010). We assumed a TPM model with a proportion of one-step mutations of 90% and an average size of non-one-step mutations of 3.5 (Garza & Williamson 2001).

MSVAR method. To detect and quantify changes in N_e , we used a method relying on a hierarchical Bayesian model based on a coalescent framework (as implemented in MSVAR 1.3, Beaumont 1999; Storz & Beaumont 2002). This model assumes that a stable, closed population of ancestral size N_1 increased or decreased exponentially to its current size N_0 over a time interval ta (in years). Given lognormal prior distributions and microsatellite data (i.e. allelic distribution and relative allele sizes), the method infers the model parameters $\Phi = \{N_0, N_1, ta, \theta\}$, where $\theta = 4N_0\mu$ and μ is the mutation rate. The posterior probability density of Φ is established through Markov chain Monte Carlo (MCMC) techniques. Loci are supposed to be independent and to evolve under a strict SMM, but the method is also robust against deviations from strict SMM (Storz & Beaumont 2002; Girod *et al.* 2011). For each MSVAR analysis, we performed four independent runs of 5×10^9 steps, varying the starting values and means for priors and hyperpriors (values in Table S2, Supporting information). Parameters were thinned with an interval of 5×10^4 steps, resulting in output files with 1×10^5 values. To avoid bias induced by the starting values on parameter estimation, the first

10% of the chains were discarded (i.e. burn-in). We checked the convergence of the chains visually and with the Gelman and Rubin analysis (Gelman & Rubin 1992). We considered that chains converged well when values smaller than 1.1 were obtained (Gelman & Hill 2007).

For each independent run of MSVAR, the magnitude of the demographic change was estimated through the calculation of an effect size (i.e. Hedges' d , Hedges & Olkin 1985) and its 95% confidence interval. Hedges' d is a mean standardized difference (i.e. independent of the original scale) between the log of the ancestral population size [$\log(N_1)$] and the log of the current population size [$\log(N_0)$]. The standardization of the mean difference is obtained by dividing the mean difference by a pooled standard deviation (formulas in Appendix S1, Supporting information). We combined the four effect sizes of each independent run to calculate a mean effect size (MES) *per* analysis, along with its 95% confidence interval (Rosenberg *et al.* 1997). A MES value whose confidence interval includes zero means that the population did not experience a significant demographic change. Significantly negative values correspond to significant bottlenecks, while significantly positive values are significant population expansions. Pairs of MES were considered as significantly different when their 95% confidence intervals did not overlap. Information about these methods along with an illustrative example is provided in the Appendix S1 (Supporting information).

For empirical data, we further estimated the beginning of the exponential demographic changes inferred with MSVAR by calculating Bayes' factors (BFs), which measure the weight of evidence of alternative time intervals for ta (i.e. the time of the beginning of the demographic change). BFs were first computed for time periods of 10 years in a sliding window from 0 to 100 years, then for periods of 100 years from 200 to 10 000 years ago. BFs greater than 4 are usually interpreted as positive evidence, while BFs >7 are considered as significant (Storz & Beaumont 2002; Sousa *et al.* 2008). For each species on the highly fragmented river, we also calculated (through the posterior distribution of ta) the probability that the detected demographic changes occurred (i) after dam construction ($p_{(\text{dam})}$, ta between 0–60 years ago) and (ii) after weir construction began ($p_{(\text{weir})}$, ta between 0–800 years ago). We considered a generation time of three years for *S. cephalus* and *L. burdigalensis* and of two years for *G. gobio* and *P. phoxinus* (Poncin *et al.* 1987). For the sake of clarity, we present only BFs computed for ta at the population level.

Effects of N , m , a and distance from the source on demographic history inference. In order to synthesize results obtained from the simulated data sets, we ran generalized linear models (GLMs) to statistically test for each

method independently the effects of N , m , a and distance from the putative source (D) on inferences of changes in N_e . In these models, the dependent variables were ΔH , M and MES (calculated at the deme level) for the BOTTLENECK, M-ratio and MSVAR methods, respectively. Explanatory variables were N , m , a and D . They were all treated as fixed effects, and we further included all two-term and three-term interactions so as to test the significance of interacting effects between explanatory variables. We assumed Gaussian error terms for all dependent variables, and the significance of each fixed effect was assessed using F-ratio tests.

Results

Simulated data

BOTTLENECK method. At the deme level and over all scenarios, 47 data sets (47/270 = 17.4%) exhibited significant departures from mutation–drift equilibrium. Most of them (32/47 = 68%) displayed significant heterozygosity deficiencies, which are generally interpreted as signals of demographic expansions. Only 15 demes displayed significant heterozygosity excesses, which are generally interpreted as signals of bottlenecks. At the population level, and over all scenarios, we detected 14 (14/27 = 51.9%) significant departures from mutation–drift equilibrium, all in the form of heterozygosity deficiencies. Additionally, our GLM-based analysis revealed a significant three-way interaction between N , m and a (Table 1). This analysis indicates that the BOTTLENECK method detected false signals of expansion (i.e. negative values of ΔH) under moderate (i.e. $a = 7.5$) and strong (i.e. $a = 50$) gene flow asymmetries, although this pattern was altered by the effective population size at the deme level (Fig. 2A–C).

M-ratio method. At the deme level and over all scenarios, 36.3% of the demes (i.e. 98/270) displayed a significant signal of population decrease. However, at the population level, no significant signals of demographic decline were detected. The GLM-based analysis also highlighted a significant three-way interaction between N , m and a (Table 1). This analysis confirmed that the M-ratio method detected false signals of bottlenecks, but only for symmetric gene flow, and under some specific combinations of N and m (Fig. 2D).

MSVAR method. 41.85% of deme-level data sets (i.e. 113/270) indicated significant signals of demographic change. Among these significant signals, false signals of expansion were more frequent than false signals of bottleneck (69% vs. 31%, respectively). According to the GLM analysis, we detected two significant two-term interactions,

Table 1 Results for the generalized linear models used to synthesize results obtained from the analyses of simulated data sets with (i) BOTTLENECK (associated dependent variable = ΔH), (ii) the M-ratio method (i.e. M) and (iii) MSVAR [i.e. mean effect size (MES)]

Explanatory variables	Dependent variables		
	ΔH	M	MES
Distance from the source (D)	NS	NS	***
Effective population size (N)	***	***	***
Migration rate (m)	***	***	NS
Asymmetry coefficient (a)	***	***	*
$D*N$	NS	**	NS
$D*m$	NS	NS	NS
$D*a$	NS	NS	NS
$N*m$	***	***	**
$m*a$	**	**	***
$N*a$	***	***	NS
$D*N*m$	NS	NS	NS
$D*m*a$	NS	NS	NS
$D*N*a$	NS	NS	NS
$N*m*a$	**	***	NS

NS indicates P -values > 0.05 ; *indicates P -values < 0.05 ; **indicates P -values < 0.01 ; ***indicates P -values < 0.001 . Significant effects indicate that explanatory variables significantly affect one of the three dependent variables, each being related to one of the three methods used to infer demographic changes. Significant single terms are not interpreted when they are involved in significant interaction terms.

one implying N and m and the other implying m and a (Table 1). The first interaction indicated that, irrespective of a , false signals of bottleneck were mainly detected for low values of N and m , whereas false signals of expansion tended to be greater for intermediate values of m (0.053) and large values of N (> 500 , Fig. 3A). The second interaction indicates that, irrespective of N , strong signals of false bottlenecks were mainly detected for situations of symmetric gene flow (i.e. $a = 1$), but only for low migration rate ($m = 0.01$, Fig. 3B). In contrast, strong signals of false expansions were detected under several and contrasted combinations of m and a (Fig. 3B). Indeed, false signals of expansion were detected under symmetric gene flow and with high migration rate ($m = 0.1$), but also under asymmetric gene flow ($a = 7.5$ or 50) and low to medium migration rates ($m = 0.01$ or 0.053 , Fig. 3B). We additionally found that, overall, the magnitude of the false demographic expansion increased with the distance from the putative source (Table 1).

Empirical data

BOTTLENECK method. At the sampling site level, we detected a significant heterozygosity excess in only one

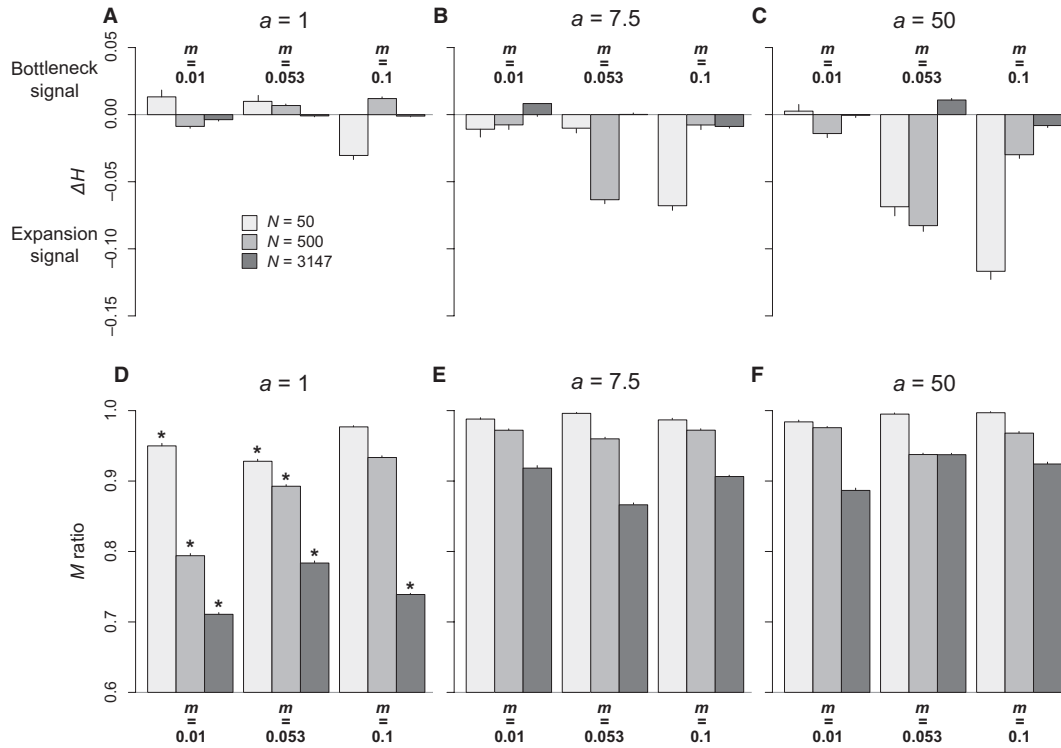


Fig. 2 Barplots representing values of ΔH (A, B and C) and M (D, E and F) in function of three interacting parameters (as revealed by the GLM-approach: N , m and a). Vertical lines correspond to the standard error. *means that the population has experienced a significant bottleneck (i.e. $M < M_c$).

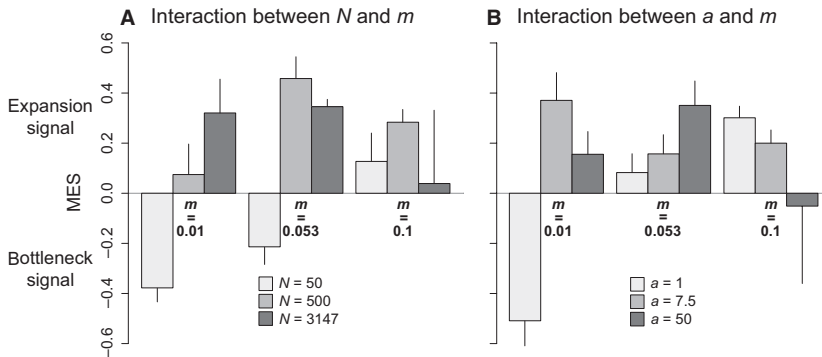


Fig. 3 Barplots representing values of mean effect sizes (MES) in function of two different two-term interactions (as revealed by the GLM approach): (A) interaction between the parameters N and m and (B) interaction between m and a . Vertical lines correspond to the standard error.

case (i.e. site V8 for *Squalius cephalus* in the River Viaur, Table S3, Supporting information). In contrast, 17 significant heterozygosity deficiencies were detected (Table S3, Supporting information). None of these deviations were significant after Bonferroni corrections. In contrast, at the population level, significant heterozygosity deficiencies were found for all species and in the two rivers (Table 2).

M-ratio method. At the sampling site level, the M-ratio test detected significant bottlenecks at all sites, irrespective of the species and the river (Table S3, Supporting

information). At the population level, all populations exhibited significant signals of bottleneck but one (i.e. *G. gobio* in the river Célé; Table 2).

MSVAR method. At the sampling site level, most sampling sites displayed significant bottlenecks (i.e. all MES values were significantly negative), a pattern that holds true for all species and rivers (Fig. 4). There were no clear spatial patterns along the upstream–downstream gradient (i.e. demographic changes did not tend to be larger either downstream or upstream, Fig. 4). However, there were striking site-to-site MES discrepancies.

Table 2 Results for the Wilcoxon's sign rank tests computed by BOTTLENECK for the empirical data and for the M-ratio test. For the two methods, analyses were conducted at the population level assuming a two-phase mutation model (TPM) mutation model

Species	River	Status	Wilcoxon excess	Wilcoxon deficiency	M (SD)
<i>Squalius cephalus</i>	Viaur	Highly fragmented	0.997NS	0.005 [†]	0.571 (0.217) [‡]
<i>Leuciscus burdigalensis</i>	Viaur	Highly fragmented	0.999NS	0.002 [†]	0.563 (0.197) [‡]
<i>Gobio gobio</i>	Viaur	Highly fragmented	0.996NS	0.006 [†]	0.6931 (0.233) [‡]
<i>Phoxinus phoxinus</i>	Viaur	Highly fragmented	0.980NS	0.027*	0.748 (0.165) [‡]
<i>Squalius cephalus</i>	Célé	Weakly fragmented	0.999NS	0.001 [†]	0.5839 (0.146) [‡]
<i>Leuciscus burdigalensis</i>	Célé	Weakly fragmented	0.999NS	<0.001 [†]	0.664 (0.203) [‡]
<i>Gobio gobio</i>	Célé	Weakly fragmented	0.980NS	0.027*	0.788 (0.201)
<i>Phoxinus phoxinus</i>	Célé	Weakly fragmented	1.000NS	0.008*	0.739 (0.171) [‡]

For the BOTTLENECK analyses: *indicates a significant deviation from mutation–drift equilibrium (P -value ≤ 0.05); [†]indicates a significant deviation from mutation–drift equilibrium after sequential Bonferroni corrections for all populations, and NS means that there is not a significant deviation from mutation–drift equilibrium (P -value > 0.05). Significant H_e excesses are evidences of recent population decreases. Significant H_e deficiencies can be interpreted as evidences of recent demographic expansion. For the M-ratio test:

[‡]indicates a significant M value (i.e. $M \leq M_c$), which is interpreted as a significant signal of population decrease, and NS means that the test is not significant (i.e. $M > M_c$).

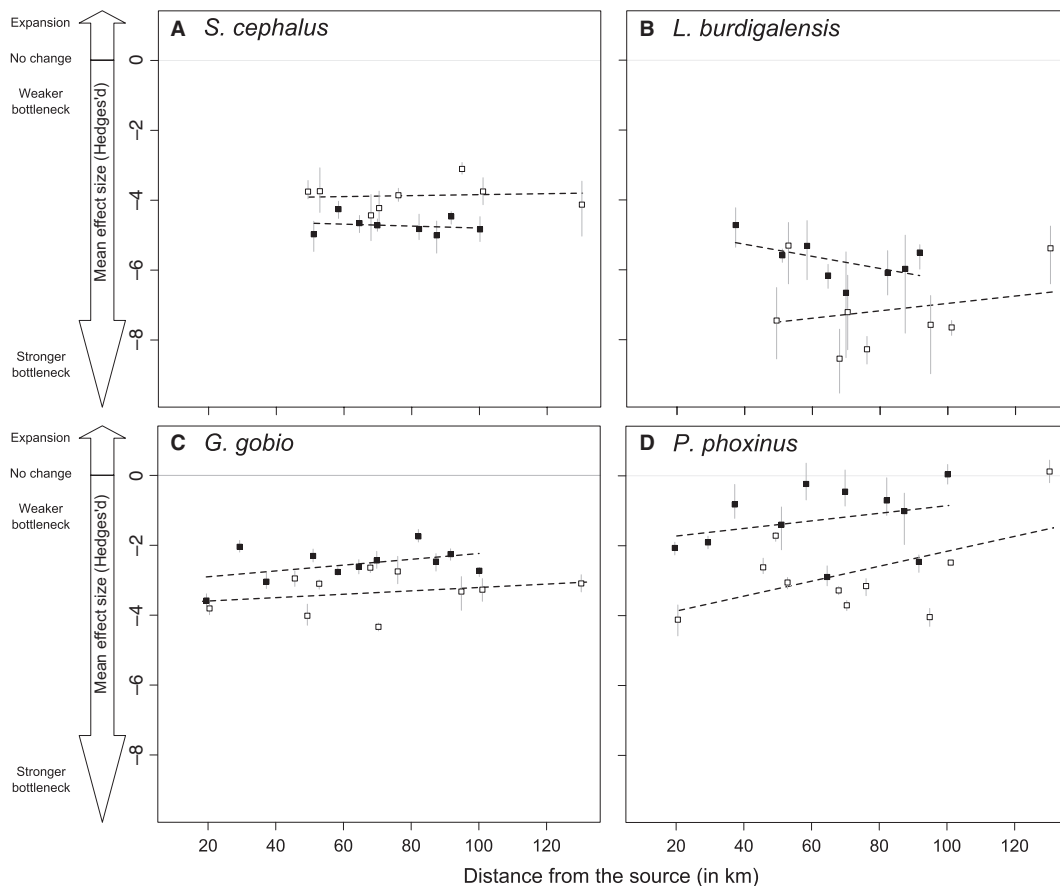


Fig. 4 Sampling site-level mean effect sizes (MES) calculated for all species and rivers. Black squares characterize the weakly fragmented river (Célé) sites, while white squares represent highly fragmented river's sites (Viaur). Dashed lines represent the nonsignificant relationships between MES values and the distance from the source at each site determined by generalized linear models (GLMs). Grey vertical lines represent MES' 95% confidence intervals (CIs). MES whose CIs include zero means that no significant demographic changes have been detected. Negative values correspond to significant bottlenecks. Intrariver and intraspecific MES can be easily compared by seeing whether their respective CIs overlap. Two MES are considered significantly different when their CIs did not overlap.

For instance, for *P. phoxinus*, we found no significant demographic changes in downstream sites for both the Célé and Viaur rivers (i.e. the MES 95% CI included 0), while other sites were characterized by signals of bottlenecks of diverse magnitudes (Fig. 4D).

Concerning population-level analyses, we found significant bottlenecks for all species and rivers (Fig. 5). These analyses indicated that the magnitude of the bottleneck tended to be stronger for the two largest species (*S. cephalus* and more particularly *L. burdigalensis*) than for the two smallest species (*G. gobio* and *P. phoxinus*, Fig. 5). Furthermore, the magnitude of the bottleneck was significantly stronger in the highly fragmented river for *L. burdigalensis* and *G. gobio* (Fig. 5).

Regarding the dating of the detected bottlenecks, we estimated that they most probably occurred more than 800 years ago (Fig. 6) and thus before dam or weir construction. Accordingly, the probabilities that these bottlenecks occurred after dam or weir construction on the highly fragmented river were very low for all species ($p_{(dam)} < 0.007$, $p_{(weir)} < 0.052$). Only *P. phoxinus* showed a non-negligible $p_{(weir)}$ of 0.238. Over all species, the population declines tended to be more ancient in the highly fragmented river than in the weakly

fragmented river, except for *L. burdigalensis* (Fig. 6). At the intrariver level, *ta* estimations were also congruent for all species but *L. burdigalensis*. This species revealed the most ancient *ta* values on the weakly fragmented river (Fig. 6A), whereas it showed one of the most recent bottlenecks on the highly fragmented river (Fig. 6B).

Discussion

As expected, our simulated data showed that asymmetric gene flow can bias the genetically based inference of past demographic changes. We notably demonstrated

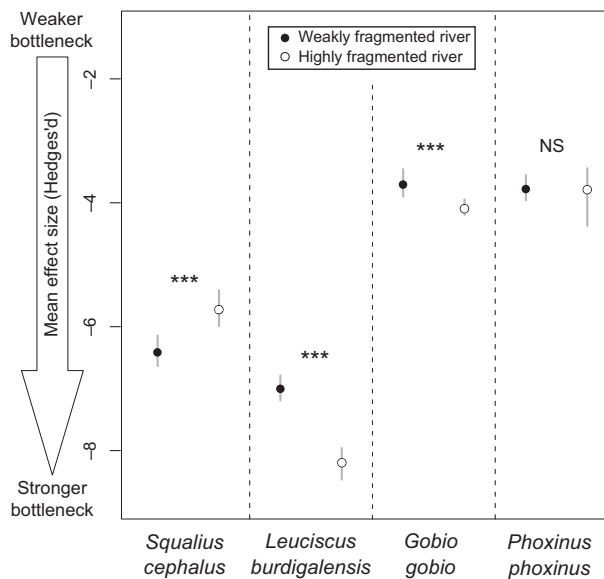


Fig. 5 Mean effect sizes (MES) for all species and rivers calculated at the population level. Grey vertical lines represent MES' 95% confidence intervals (CIs). Two MES are considered significantly different if their CIs did not overlap. Here, we symbolized only the significance of intraspecific comparisons (i.e. comparison between MES of the highly fragmented vs. the weakly fragmented river for a single species). NS indicates no significant intraspecific difference between weakly fragmented vs. highly fragmented river and ***means significant difference.

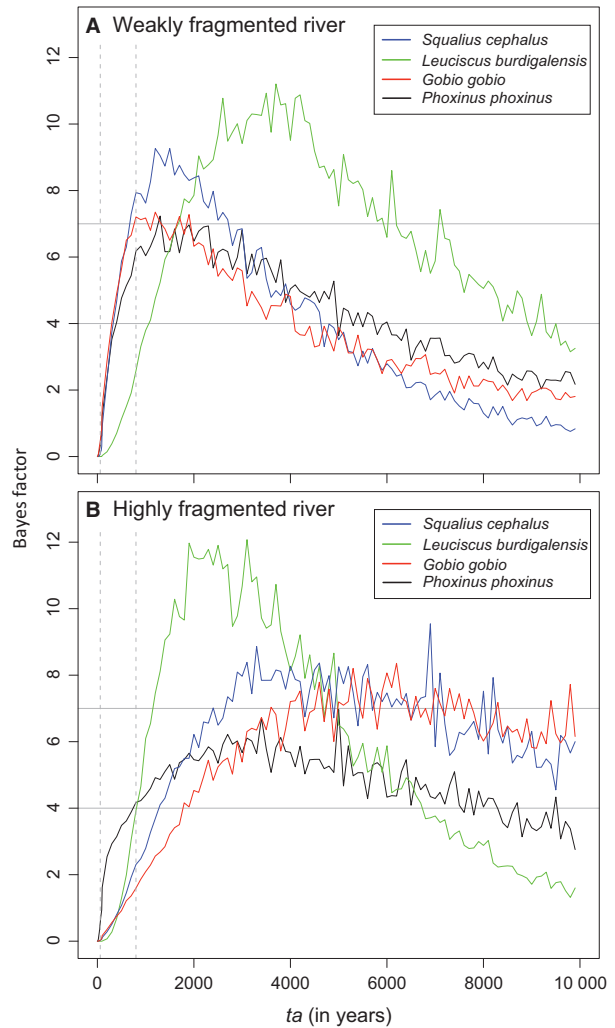


Fig. 6 Bayes' factors (BFs) for the time of the beginning of the demographic changes (*ta*) calculated for the four species for the weakly fragmented river (A) and the highly fragmented river (B). Results correspond to the population-level analyses. BFs >4 are considered as 'positive evidences', while BFs >7 are considered as significant. Dashed vertical lines correspond to the construction of dams (*ta* = 60 years) and to the beginning of weir construction (*ta* = 800 years).

that asymmetric gene flow can – under certain conditions of migration rate and effective population size – generate false signals of population expansion. Interestingly, this tendency was detected in our empirical data, but only for one of the three inference methods we used. In contrast, the other two methods revealed strong signals of bottleneck for the four fish species and across the two rivers sampled, which are characterized by different levels of asymmetric gene flow (see Table S1, Supporting information).

Effects of gene flow asymmetry on demographic history inferences

In most cases of significant – although spurious – demographic change, our simulations showed that asymmetric gene flow generates false signals of demographic expansion. However, this pattern was sensitive to other population parameters, namely the migration rate and the effective population size. We indeed detected strong interactive effects of these population parameters on signals of false demographic change. These interactive effects are yet difficult to biologically interpret, and make difficult to withdraw general predictions about the effect of asymmetric gene flow on estimates of historical demographic changes in natural systems. Our results hence demonstrate the importance of simultaneously considering multiple parameters such as the effective population size and the migration rate when testing the robustness of analytical methods through simulations.

The effect of asymmetric gene flow on demographic change inferences was also dependent on the method we used. Indeed, contrary to the *MSVAR* and the *BOTTLENECK* methods, the *M-ratio* method was not affected by asymmetric gene flow, as we found no clear evidence that downstream-biased asymmetric gene flow led to false signals of bottleneck. However, under conditions of symmetric gene flow, the *M-ratio* method tended to detect false signals of bottleneck, especially under low to moderate migration rates. As demonstrated previously for the *MSVAR* method (Chikhi *et al.* 2010), this may be due to the confounding effects of population structure and of the sampling scheme on the representativeness of genetic diversity.

We further observed correlations between distance from the upstream deme and the magnitude of the demographic expansion (only for the *MSVAR* method). These differences between upstream and downstream demes are probably the result of a source–sink dynamic, whereby downstream demes act as sinks and receive an excess of alleles through downstream-directed migration (Kawecki & Holt 2002; Morrissey & de Kerckhove 2009). Such source–sink dynamics

generally lead to a gradual increase in allelic richness along the upstream–downstream gradient in rivers (Hänfling & Weetman 2006; Blanchet *et al.* 2010) and may therefore produce signals similar to those generated by demographic expansions. This may be because the number and frequencies of alleles actually observed in downstream sites are different than what expected under a demographically stable model. Finally, we found that the symmetric gene flow scenario led to patterns of false bottlenecks (only for low migration rate), as expected from previous simulations in *n-island* and two-dimensional stepping-stone models (Städler *et al.* 2009; Chikhi *et al.* 2010).

Effect of asymmetric gene flow on fish population demographic histories

We detected significant population bottlenecks for all species in the two rivers when we analysed the empirical data. Because two of the three methods (*MSVAR* and *M-ratio* methods) were concordant in highlighting significant bottlenecks, we could reasonably assume that these populations had actually experienced demographic declines. However, significant signals of expansions were identified for all species and rivers at the population level using the *BOTTLENECK* method. This result is consistent with that obtained for the simulated data (see above), suggesting that, in wild populations, this method may be subjected to the type of bias induced by asymmetric gene flow. Overall, this would suggest that, although asymmetric gene flow may theoretically affect the inference of demographic changes (our simulations), some inference methods may be powerful enough to bypass this type of bias when a population has actually experienced a bottleneck.

We tested such a hypothesis by running an additional analysis in which we simulated a scenario where the population was subjected to (i) a bottleneck of magnitude and timing similar to that estimated for the empirical data and (ii) postbottleneck ϕ values equal to the mean values estimated from the literature survey (i.e. $N = 3147$, $a = 7.5$, $m = 0.053$). We found that *MSVAR* detected a significant bottleneck (results not shown), which suggests that at least under some conditions, *MSVAR* can bypass the bias induced by asymmetry. It is noteworthy that we also detected a significant bottleneck using the *M-ratio* test, whereas *BOTTLENECK* detected a significant heterozygosity deficiency (i.e. a population expansion signal). Regarding our empirical data, we note, however, that some sampling sites did not display significant demographic changes. For instance, the absence of significant bottlenecks for *P. phoxinus* in downstream sites suggests that asymmetric gene flow was probably strong enough in these sites

to counterbalance the effect of ancient bottlenecks. This means that more simulations varying both asymmetric gene flow and the characteristics (i.e. magnitude, date and type) of demographic changes are required to refine the conditions under which *MSVAR* adequately detects population size changes.

To summarize, our study suggests that the *BOTTLENECK* method may be less suited than the *MSVAR* and *M-ratio* methods to infer demographic changes in wild populations experiencing asymmetric gene flow. This conclusion is apparently solid, because our empirical data set includes fish populations covering a wide range of values regarding their levels of asymmetric gene flow (i.e. $1.893 < a < 9.135$), migration rate (i.e. $0.042 < m < 0.078$) and effective population size (i.e. $546.488 < N < 8088.188$; see Table S1, Supporting information). But, given the fact we do not know the actual demographic history of these populations, we should remain cautious. An important lesson from this is perhaps that each method looks at the genetic data from a slightly different angle and uses different aspects of genetic diversity measures, which may in the end mean that the methods could be used jointly once we better understand their joint properties.

From a biological point of view, we surprisingly found that the dating of the bottlenecks experienced by these populations was similar for three of the four species. For all species, we found that the corresponding demographic declines were ancient and pre-dated the construction of the weirs and dams. For the highly fragmented river, the most likely inferred dates for the beginning of the bottlenecks range from 2000 to 8000 years ago, which contrasts with the first known mill weirs in this river (~800 years ago). Such dating suggests that these bottlenecks occurred after the last glacial period (i.e. Würm glacial period, $ta < 10\,000$ years), more precisely between the Atlantic and the middle Subatlantic chronozones of the Holocene (Mangerud *et al.* 1974). These important bottlenecks might have been generated by different events, such as postglacial colonization (Hänfling *et al.* 2002; Swatdipong *et al.* 2010), environmental stochastic events or random catastrophes (Hedrick & Miller 1992; Lande 1993). The dating obtained with the *MSVAR* method might only be loosely related to any particular event. Improving our knowledge in the paleoenvironmental history of the studied region would certainly help in understanding the potential causes of such strong population declines. Moreover, in the case of a series of expansions and contractions (which are likely to have happened in many natural systems), it is unclear which event would be 'identified' by *MSVAR* (Quéméré *et al.* 2012; Salmona *et al.* 2012). Simulation of multiple events may thus be necessary for improving our interpretation of *MSVAR* outputs.

Conclusion

Recent years have shown that several factors can play significant roles in producing nonequilibrium patterns, such as isolation by distance (Leblois *et al.* 2006), population structure (Städler *et al.* 2009; Chikhi *et al.* 2010; Peter *et al.* 2010), rapid decreases in gene flow (i.e. fragmentation, Broquet *et al.* 2010), spatial expansions (Edmonds *et al.* 2004) or departures from the assumed mutation model (Chikhi *et al.* 2010). However, the consequences of asymmetrical gene flow have been neglected. Our simulations confirm our expectation that asymmetric gene flow may generate biases when inferring demographic changes from genetic data. However, the direction and magnitude of such biases depended upon other population characteristics such as migration rate and effective population size. This study demonstrates the complexity of inferring demographic changes from genetic data in wild populations and the importance of integrating multiple parameters in simulations aiming at testing the robustness of inference methods in population genetics (e.g. Heller *et al.* in press).

In spite of these potential biases, our multispecific empirical data suggest that, if used with care and conjointly, most inference methods appear suitable to infer demographic changes in populations experiencing asymmetric gene flow. Indeed, our empirical data suggest that asymmetric gene flow was unlikely to have caused the bottlenecks observed in the eight wild fish populations. We also found that if a major bottleneck was responsible of the patterns observed, it was unlikely to have been caused by recent anthropogenic fragmentation. However, we cannot claim that we have identified unambiguously the factors generating the strong bottlenecks observed in all fish species, even if they dated around the same period.

The last twenty years have seen major improvements in population genetics inference, in particular with the development of full-likelihood methods. Our results and those from previous studies clearly demonstrate that population structure and dispersal patterns have to be considered for properly inferring the demographic history of wild populations (Chikhi *et al.* 2010; Girod *et al.* 2011). An important step for future studies will be to quantify the ability of emerging methods (such as those based on approximate Bayesian computations) to efficiently disentangle signals of demographic changes from false signals arising from population structure (see Peter *et al.* 2010 for instance).

Acknowledgements

We thank Éric Petit, Thomas Broquet, Vincent Dubut, Jérôme Chave, Camille Pagès, Guillaume Evanno, Raphael Leblois and

three anonymous reviewers for their constructive and stimulating comments. Olivier Rey, Gaël Grenouillet, Loïc Tudesque, Muriel Gevrey, Laetitia Buisson, Sébastien Brosse, Leslie Faggiano and Fabien Leprieur are thanked for their help in the field. We also thank the CALMIP group, in particular Boris Dintrans and Nicolas Renon. This work was performed using high performance computing (HPC) resources from CALMIP (allocation 2010-P1003). We are grateful to Radika Michniewicz for correcting and editing the English. The authors also thank the 'Agence de l'Eau Adour-Garonne' for financial support and the 'Génopole Toulouse' for help with genotyping. This study is part of the European project 'IMPACT'. This project has been carried out with financial support from the Commission of the European Communities, specific RTD program 'IWRMNET'. IP is financially supported by a MESR ('Ministère de l'Enseignement Supérieur et de la Recherche') PhD scholarship. This work has been carried out in two research units (EDB & EcoEx CNRS Moulis) that are part of the 'Laboratoire d'Excellence' (LABEX) entitled TULIP (ANR-10-LABX-41).

References

- Aljanabi SM, Martinez I (1997) Universal and rapid salt-extraction of high quality genomic DNA for PCR-based techniques. *Nucleic Acids Research*, **25**, 4692–4693.
- Alò D, Turner TF (2005) Effects of habitat fragmentation on effective population size in the endangered Rio Grande silvery minnow. *Conservation Biology*, **19**, 1138–1148.
- Beaumont MA (1999) Detecting population expansion and decline using microsatellites. *Genetics*, **153**, 2013–2029.
- Beaumont MA, Zhang WY, Balding DJ (2002) Approximate Bayesian computation in population genetics. *Genetics*, **162**, 2025–2035.
- Blanchet S, Rey O, Etienne R, Lek S, Loot G (2010) Species-specific responses to landscape fragmentation: implications for management strategies. *Evolutionary Applications*, **3**, 291–304.
- Bolland JD, Cowx IG, Lucas MC (2008) Movements and habitat use of wild and stocked juvenile chub, *Leuciscus cephalus* (L.), in a small lowland river. *Fisheries Management and Ecology*, **15**, 401–407.
- Broquet T, Angelone S, Jaquiere J *et al.* (2010) Genetic bottlenecks driven by population disconnection. *Conservation Biology*, **24**, 1596–1605.
- Chikhi L, Bruford MW (2005) Mammalian population genetics and genomics. In: *Mammalian Genomics* (eds Ruvinsky A, Marshall Graves J), pp. 539–583. CABI Publishing, CAB International, Wallingford, Oxfordshire, UK. Chapter 21.
- Chikhi L, Sousa VC, Luisi P, Goossens B, Beaumont MA (2010) The confounding effects of population structure, genetic diversity and the sampling scheme on the detection and quantification of population size changes. *Genetics*, **186**, 983–995.
- Cornuet JM, Luikart G (1996) Description and power analysis of two tests for detecting recent population bottlenecks from allele frequency data. *Genetics*, **144**, 2001–2014.
- Csillery K, François O, Blum MGB (2012) ABC: an R package for approximate Bayesian computation (ABC). *Methods in Ecology and Evolution*, **3**, 475–479.
- De Leeuw JJ, Winter HV (2008) Migration of rheophilic fish in the large lowland rivers Meuse and Rhine, the Netherlands. *Fisheries Management and Ecology*, **15**, 409–415.
- Di Rienzo A, Peterson AC, Garza JC *et al.* (1994) Mutational processes of simple-sequence repeat loci in human populations. *Proceedings of the National Academy of Sciences of the United States of America*, **91**, 3166–3170.
- Edmonds CA, Lillie AS, Cavalli-Sforza LL (2004) Mutations arising in the wave front of an expanding population. *Proceedings of the National Academy of Sciences of the United States of America*, **101**, 975–979.
- Fahrig L (2003) Effects of habitat fragmentation on biodiversity. *Annual Review of Ecology Evolution and Systematics*, **34**, 487–515.
- Garza JC, Williamson EG (2001) Detection of reduction in population size using data from microsatellite loci. *Molecular Ecology*, **10**, 305–318.
- Gelman A, Hill J (2007) *Data Analysis using Regression and Multilevel/Hierarchical Models*. Cambridge University Press, New York.
- Gelman A, Rubin DB (1992) Inference from iterative simulation using multiple sequences. *Statistical Science*, **7**, 457–472.
- Girod C, Vitalis R, Leblois R, Freville H (2011) Inferring population decline and expansion from microsatellite data: a simulation-based evaluation of the msvar method. *Genetics*, **188**, 165–179.
- Goossens B, Chikhi L, Ancrenaz M *et al.* (2006) Genetic signature of anthropogenic population collapse in orang-utans. *PLoS Biology*, **4**, 285–291.
- Hänfling B, Weetman D (2006) Concordant genetic estimators of migration reveal anthropogenically enhanced source-sink population structure in the River Sculpin, *Cottus gobio*. *Genetics*, **173**, 1487–1501.
- Hänfling B, Hellemans B, Volckaert FAM, Carvalho GR (2002) Late glacial history of the cold-adapted freshwater fish *Cottus gobio*, revealed by microsatellites. *Molecular Ecology*, **11**, 1717–1729.
- Hanski I (1998) Metapopulation dynamics. *Nature*, **396**, 41–49.
- Hedges LV, Olkin I (1985) *Statistical Methods for Meta-Analysis*. Academic Press, New York.
- Hedrick PW, Miller PS (1992) Conservation genetics – Techniques and fundamentals. *Ecological Applications*, **2**, 30–46.
- Heller R, Chikhi L, Sigismund HR (2013) The confounding effect of population structure on Bayesian skyline plot inferences of demographic history. *PLoS One* (in press), e62992, doi:10.1371/journal.pone.0062992.
- Henle K, Lindenmayer DB, Margules CR, Saunders DA, Wissel C (2004) Species survival in fragmented landscapes: where are we now? *Biodiversity and Conservation*, **13**, 1–8.
- Hoban S, Bertorelle G, Gaggiotti OE (2012) Computer simulations: tools for population and evolutionary genetics. *Nature Reviews Genetics*, **13**, 110–122.
- Horreo JL, Martinez JL, Ayllon F *et al.* (2011) Impact of habitat fragmentation on the genetics of populations in dendritic landscapes. *Freshwater Biology*, **56**, 2567–2579.
- Hudson RR (2002) Generating samples under a Wright-Fisher neutral model of genetic variation. *Bioinformatics*, **18**, 337–338.
- Kawecki TJ, Holt RD (2002) Evolutionary consequences of asymmetric dispersal rates. *American Naturalist*, **160**, 333–347.
- Kingman JFC (1982) On the genealogy of large populations. *Journal of Applied Probability*, **19**, 27–43.
- Lande R (1993) Risks of population extinction from demographic and environmental stochasticity and random catastrophes. *American Naturalist*, **142**, 911–927.

- Leblois R, Estoup A, Streiff R (2006) Genetics of recent habitat contraction and reduction in population size: does isolation by distance matter? *Molecular Ecology*, **15**, 3601–3615.
- Mangerud J, Andersen ST, Berglund BE, Donner JJ (1974) Quaternary stratigraphy of Norden, a proposal for terminology and classification. *Boreas*, **3**, 109–126.
- Morrissey MB, de Kerckhove DT (2009) The maintenance of genetic variation due to asymmetric gene flow in dendritic metapopulations. *American Naturalist*, **174**, 875–889.
- Nielsen R, Beaumont MA (2009) Statistical inferences in phylogeography. *Molecular Ecology*, **18**, 1034–1047.
- Nock CJ, Overden JR, Butler GL *et al.* (2011) Population structure, effective population size and adverse effects of stocking in the endangered Australian eastern freshwater cod *Maccullochella ikei*. *Journal of Fish Biology*, **78**, 303–321.
- Peter BM, Wegmann D, Excoffier L (2010) Distinguishing between population bottleneck and population subdivision by a Bayesian model choice procedure. *Molecular Ecology*, **19**, 4648–4660.
- Piry S, Luikart G, Cornuet JM (1999) BOTTLENECK: a computer program for detecting recent reductions in the effective population size using allele frequency data. *Journal of Heredity*, **90**, 502–503.
- Pollux BJA, Luteijn A, Van Groenendael JM, Ouborg NJ (2009) Gene flow and genetic structure of the aquatic macrophyte *Sparganium emersum* in a linear unidirectional river. *Freshwater Biology*, **54**, 64–76.
- Poncin P, Melard C, Philippart JC (1987) Use of temperature and photoperiod in the control of the reproduction of 3 European cyprinids, *Barbus barbus* (L.), *Leuciscus cephalus* (L) and *Tinca tinca* (L), reared in captivity – Preliminary Results. *Bulletin Français De La Pêche Et De La Pisciculture*, **304**, 1–12.
- Quéméré E, Amelot X, Pierson J, Crouau-Roy B, Chikhi L (2012) Genetic data suggest a natural pre-human origin of open habitats in northern Madagascar and question the deforestation narrative in this region. *Proceedings of the National Academy of Sciences of the United States of America*, **109**, 13028–13033.
- Raeymaekers JAM, Maes GE, Geldof S *et al.* (2008) Modelling genetic connectivity in sticklebacks as a guideline for river restoration. *Evolutionary Applications*, **1**, 475–488.
- Rosenberg MS, Adams DC, Gurevitch J (1997) *Metawin: Statistical Software for Meta-Analysis with Resampling Tests*. Sinauer Associates, Sunderland, Massachusetts, iv, 65.
- Salmona J, Salamolard M, Fouillot D *et al.* (2012) Signature of a pre-human population decline in the critically endangered reunion island endemic forest bird *Coracina newtoni*. *PLoS One*, **7**(8), e43524.
- Sousa V, Penha F, Collares-Pereira MJ, Chikhi L, Coelho MM (2008) Genetic structure and signature of population decrease in the critically endangered freshwater cyprinid *Chondrostoma lusitanicum*. *Conservation Genetics*, **9**, 791–805.
- Städler T, Haubold B, Merino C, Stephan W, Pfaffelhuber P (2009) The impact of sampling schemes on the site frequency spectrum in nonequilibrium subdivided populations. *Genetics*, **182**, 205–216.
- Storz JF, Beaumont MA (2002) Testing for genetic evidence of population expansion and contraction: an empirical analysis of microsatellite DNA variation using a hierarchical Bayesian model. *Evolution*, **56**, 154–166.
- Swatdipong A, Primmer CR, Vasemagi A (2010) Historical and recent genetic bottlenecks in European grayling, *Thymallus thymallus*. *Conservation Genetics*, **11**, 279–292.
- Weiss G, von Haeseler A (1998) Inference of population history using a likelihood approach. *Genetics*, **149**, 1539–1546.
- Yue GH, David L, Orban L (2007) Mutation rate and pattern of microsatellites in common carp (*Cyprinus carpio* L.). *Genetica*, **129**, 329–331.

Data accessibility

R scripts for analysing *MSVAR* outputs and for simulating genetic data with *ms*, empirical microsatellite data sets and simulated microsatellite data sets are available at Dryad Digital Repository doi:10.5061/dryad.5sc31.

I.P., S.B., G.L., E.Q. and LC wrote the article. SB, IP and GL designed the study and managed the project. I.P., S.B., E.Q. and LC implemented the methods and analysed the results. All authors read and approved this version of the manuscript.

Supporting information

Additional supporting information may be found in the online version of this article.

Fig. S1 Diagram summarizing the parameter exploration procedure applied to our model.

Fig. S2 Geographic location of the “weakly fragmented” (Célé) and “highly fragmented” (Viaur) rivers.

Table S1 Mean allelic richness (*AR*) and Pearson’s correlation coefficient values (*r*) obtained or computed for several populations from a literature survey, along with median values for *N*, *m* and *a* estimated through ABC-regression algorithms for each population.

Table S2 Starting values for priors and hyperpriors for the four *MSVAR* MCMC independent runs.

Table S3 Results for the Wilcoxon’s sign rank test computed by Bottleneck for each sampling site, species and river (left), along with sampling site information.

Appendix S1 Hedges’*d* effect size calculation.